

## ORIGINAL ARTICLE

## Obesity but not high-fat diet impairs lymphatic function

GD García Nores<sup>1</sup>, DA Cuzzone<sup>1</sup>, NJ Albano, GE Hespe, RP Kataru, JS Torrisi, JC Gardenier, IL Savetsky, SZ Aschen, MD Nitti and BJ Mehrara

**BACKGROUND/OBJECTIVES:** High-fat diet (HFD)-induced obesity has significant negative effects on lymphatic function, but it remains unclear whether this is a direct effect of HFD or secondary to adipose tissue deposition.

**METHODS:** We compared the effects of HFD on obesity-prone and obesity-resistant mice and analyzed lymphatic function *in vivo* and *in vitro*.

**RESULTS:** Only obesity-prone mice had impaired lymphatic function, increased perilymphatic inflammation and accumulation of lipid droplets surrounding their lymphatic endothelial cells (LECs). LECs isolated from obesity-prone mice, in contrast to obesity-resistant animals, had decreased expression of VEGFR-3 and Prox1. Exposure of LECs to a long-chain free fatty acid increased cellular apoptosis and decreased VEGFR-3 expression, while inhibition of intracellular inhibitors of VEGFR-3 signaling pathways increased cellular viability.

**CONCLUSIONS:** Collectively, our studies suggest that HFD-induced obesity decreases lymphatic function by increasing perilymphatic inflammation and altering LEC gene expression. Reversal of diminished VEGFR-3 signaling may rescue this phenotype and improve lymphatic function.

*International Journal of Obesity* (2016) 40, 1582–1590; doi:10.1038/ijo.2016.96

## INTRODUCTION

The incidence of obesity is rapidly rising in western countries; in the United States alone, it is estimated that 1 in 3 adults and 1 in 6 children are obese.<sup>1</sup> This is important because obesity is a significant risk factor for a variety of systemic disorders and adds nearly 200 billion dollars to our annual health-care budget.<sup>2</sup> Therefore, understanding the mechanisms that regulate obesity-related pathology is an important goal.

Chronic adipose tissue inflammation is thought to contribute to a large number of pathologic responses in obesity, including metabolic syndrome and malignancy. These responses are modulated by T cells and macrophages, leading to increased local/systemic expression of inflammatory cytokines and release of free fatty acids (FFA) with direct toxic effects on surrounding tissues.<sup>3–6</sup> In addition, adipose tissue functions as an endocrine organ that produces substances that regulate function and obesity-related pathology.<sup>5,7</sup>

Recent studies have shown that obesity has significant negative effects on the lymphatic system. For example, our group and others have shown that high-fat diet (HFD)-induced obesity markedly decreases interstitial fluid transport, immune cell trafficking and lymphatic collecting vessel pumping.<sup>8–10</sup> These negative consequences were correlated with increasing body mass, suggesting that adipose deposition has a role in this response. In contrast, others have reported that high fructose diet-induced metabolic syndrome<sup>11</sup> or hypercholesterolemia<sup>12</sup> decreases collecting vessel pumping and results in lymphatic system abnormalities independent of obesity. Thus, although it is clear that obesity can cause lymphatic dysfunction, the independent effects of dietary changes and weight gain on the lymphatic system remain unknown.

In this study, we sought to determine the independent effects of prolonged HFD intake with or without concomitant obesity on lymphatic function. By comparing the effects of HFD in obesity-

prone and obesity-resistant mice, we show that dietary changes alone are insufficient to induce lymphatic dysfunction. In addition, we show that lymphatic dysfunction in obesity-prone mice correlates with perilymphatic accumulation of inflammatory cells and lipids, and alterations in lymphatic endothelial cell (LEC) gene expression of lymphatic markers and inflammatory receptors. Finally, using correlative *in vitro* studies, we show that exposure of LECs to stearic acid (SA), a long-chain fatty acid known to be increased in obese tissues,<sup>13</sup> results in decreased VEGFR-3 expression, apoptosis and growth inhibition. Furthermore, intracellular modulation of VEGFR-3 signaling by inhibiting dephosphorylation of phosphatidylinositol 3,4,5-trisphosphate-tyrosine kinase (PIP3), addition of recombinant VEGF-C (direct activation of VEGFR-3) or recombinant insulin (indirect activation of PIP3 pathway) rescues LECs and markedly decreases apoptosis. Taken together, our findings suggest that obesity-induced inflammation, and not HFD, is responsible for the pathologic changes observed in the lymphovascular system and that these changes are due at least in part to direct injury to the LECs via by-products of inflamed adipose tissues, including long-chain FFAs.

## MATERIALS AND METHODS

An extended version of Materials and Methods is available on the *International Journal of Obesity* website.

## Animals, diets and metabolic analysis

Male C57BL/6J, BALB/cJ and lean (Ln) allele of myostatin (MSTN<sup>ln</sup>) mice were purchased from Jackson Laboratories (Bar Harbor, ME, USA) and maintained on a HFD (Purina Test Diet 60% kcal from fat; WF Fisher & Son, Inc., Somerville, NJ, USA) for 10–12 weeks. Age-matched controls on the same genetic backgrounds were maintained on a normal chow diet (NCD, 13% kcal from fat; Purina PicoLab Rodent Diet 20) for the same period of time.

Division of Plastic and Reconstructive Surgery, The Department of Surgery, Memorial Sloan Kettering Cancer Center, New York, NY, USA. Correspondence: Dr BJ Mehrara, The Department of Surgery, Memorial Sloan Kettering Cancer Center, Memorial Hospital, 1275 York Avenue, Suite MRI 1006, New York, 10065 NY, USA. E-mail: mehrarab@mskcc.org

<sup>1</sup>These authors contributed equally to this work.

Received 23 October 2015; revised 27 April 2016; accepted 2 May 2016; accepted article preview online 20 May 2016; advance online publication, 21 June 2016

### Analysis of lymphatic function

Lymphoscintigraphy was used to analyze the lymph node uptake following peripheral injection of a technetium-labeled colloid ( $^{99m}\text{Tc}$ ) as previously reported.<sup>14</sup> We used a modification of previously reported methods to analyze dendritic cell (DC) trafficking<sup>15</sup> and ferritin uptake.<sup>16</sup>

### Histology

Tissues were analyzed with immunofluorescent staining as previously reported.<sup>14</sup>

### LEC isolation and PCR

Dermal LECs were isolated from the abdominal skin by digestion in 0.4% Collagenase IV digestion buffer (MP Biomedicals, Solon, OH, USA) and flow cytometry to sort for LECs (CD45<sup>-</sup>, CD31<sup>+</sup>, podoplanin<sup>+</sup>).<sup>17</sup> RNA was extracted using TRIZOL (Invitrogen, Life Technologies, Carlsbad, CA, USA) and converted into cDNA with TaqMan reverse transcriptase kit (Roche, Branchburg, NJ, USA). Relative gene expression between groups was analyzed by normalizing gene expression with GAPDH.<sup>18</sup>

### ELISA

Protein isolated from skin/subcutaneous tissues and serum was analyzed with ELISA to quantify CCL21, IL-1 $\beta$ , TNF- $\alpha$  (Sigma-Aldrich, St Louis, MO, USA), VEGF-C (United States Biological, Salem, MA, USA) or FFA (Abcam, Cambridge, MA, USA) following the manufacturer's protocol.

### Cell culture, immunocytochemistry and western blot

Human dermal LECs and adipose-derived mesenchymal stem cells (ASCs) were obtained from PromoCell (Heidelberg, Germany) and stained in chamber slides for Prox1, Ki67 (Abcam), p-AKT (Cell Signaling Technology, Danvers, MA, USA) and VEGFR-3 (EMD Millipore, Billerica, MA, USA). Cell signal intensity was quantified using MetaMorph (Molecular Devices, Sunnyvale, CA, USA). Western blot analysis for VEGFR-3 (Abcam), p-AKT and

p-eNOS (Cell Signaling Technology) was performed with total cellular protein harvested from LECs and quantified with NIH Image J.<sup>19</sup>

### Cellular apoptosis and viability assays

Apoptosis in response to SA (0.1, 1, 10, 100  $\mu\text{M}$ ) with/without 0.3 nM Phosphatase and tensin homolog inhibitor (PTENi; SF1670, Sigma-Aldrich)<sup>20</sup> was quantified using caspase-3 assay (R&D Systems, Minneapolis, MN, USA) and Annexin V-FITC Apoptosis Detection Kit (eBioscience, San Diego, CA, USA). Viability was measured using a WST-8 cytotoxicity cell assay kit (Sigma-Aldrich).

### Statistical analysis

Statistical analysis was performed using GraphPad Prism 6 software (La Jolla, CA, USA) and differences between two groups were analyzed using a Student's *t*-test. Data are expressed as mean  $\pm$  s.d. with  $P < 0.05$  considered as significant.

## RESULTS

### HFD decreases lymphatic vascular density in obesity-prone mice

To study the effects of obesity and HFD on lymphatic function, obesity-prone C57BL/6J mice were compared with obesity-resistant BALB/c<sup>21</sup> and MSTN<sup>ln</sup> mice.<sup>22</sup> As expected, feeding male C57BL/6J mice a HFD for 10 weeks resulted in obesity characterized by marked weight gain (164% increase), ninefold increase in subcutaneous adipose deposition, mild glucose intolerance and increased fasting serum insulin levels (Figures 1a and c and Supplementary Figure 1A and B). In contrast, BALB/c mice fed a HFD gained only a small though significant amount of weight (8%), with modest increases (2.86-fold) in subcutaneous adipose tissue thickness, mildly increased

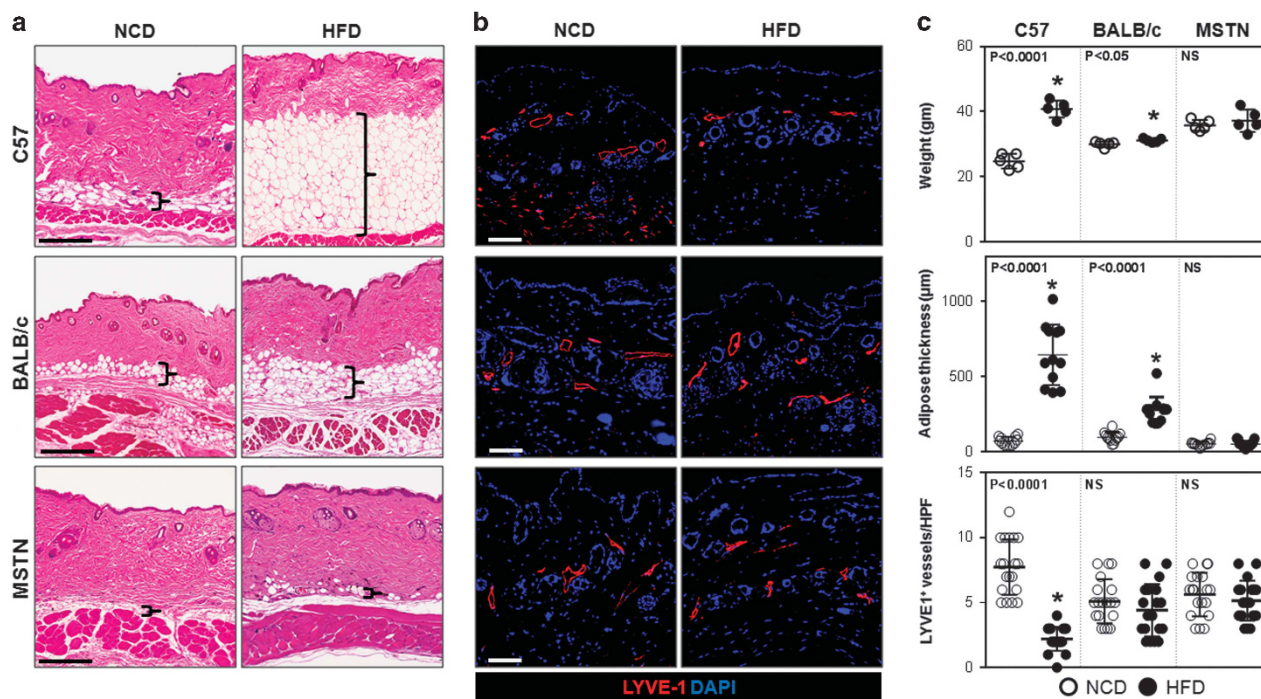


**Figure 1.** HFD results in decreased lymphatic vascular density in obesity-prone mice. **(a)** Representative H&E-stained sections of back skin from NCD- or HFD-fed C57BL/6J, BALB/cJ and MSTN<sup>ln</sup> mice (scale bar = 200  $\mu\text{m}$ ; bracket surrounds subcutaneous adipose tissues). **(b)** Representative immunofluorescent localization of LYVE-1<sup>+</sup> vessels in upper limb tissues of NCD- or HFD-fed mice in all groups (scale bar = 100  $\mu\text{m}$ ). **(c)** *Upper panel:* Body weights of mice on NCD (open circles) and HFD (filled circles) in all groups ( $n = 5/\text{group}$ ). C57BL/6J HFD vs NCD ( $*P < 0.0001$ ). BALB/cJ HFD vs NCD ( $*P < 0.05$ ). MSTN<sup>ln</sup> mice had no significant difference. *Middle panel:* Quantification of subcutaneous soft tissue thickness in NCD- and HFD-fed mice in all groups ( $n = 5-10/\text{group}$ ). C57BL/6J HFD vs NCD ( $*P < 0.0001$ ). MSTN<sup>ln</sup> and BALB/cJ mice show no significant difference between NCD and HFD groups. *Lower panel:* Quantification of upper limb LYVE-1<sup>+</sup> lymphatic vessel density per high powered field (HPF) and quadrant in NCD- and HFD-fed mice in all groups ( $n = 5 \text{ animals} \times 4\text{HPF}/\text{group}$ ). C57BL/6J HFD vs NCD ( $*P < 0.0001$ ). MSTN<sup>ln</sup> and BALB/cJ mice show no significant difference between NCD and HFD groups.

fasting serum insulin levels and no signs of glucose intolerance. HFD-fed *MSTN<sup>ln</sup>* mice remained lean throughout the study and displayed no abnormalities in glucose metabolism. All HFD-fed mice, regardless of strain, had modestly increased serum levels of total and high-density lipoprotein cholesterol and increased levels of FFA in serum; HFD-fed C57BL/6J and BALB/cJ mice also displayed increased serum low-density lipoprotein (Supplementary Figure 1C and D). HFD-induced obesity in C57BL/6J mice correlated with a decrease in lymphatic (LYVE-1<sup>+</sup>) vessel density in the dermis and subcutaneous tissues as compared with their lean NCD-fed controls (Figure 1b). In contrast, obesity-resistant HFD-fed BALB/cJ and *MSTN<sup>ln</sup>* mice demonstrated no significant differences.

#### Obesity impairs lymphatic transport

The rate of uptake and peak transport of macromolecules by the lymphatic system can be quantified by injecting <sup>99m</sup>Tc labeled sulfur colloid in the distal hindlimb and analyzing its uptake by the inguinal lymph node.<sup>14</sup> Consistent with our previous studies, analysis of lymphatic transport in HFD-fed C57BL/6J revealed significant decreases in both total and rate of lymph node <sup>99m</sup>Tc uptake (Figures 2a–c). In contrast, HFD-fed obesity-resistant mice had no significant decrease in peak or rate of <sup>99m</sup>Tc uptake as compared with their respective lean controls.

Peripherally injected ferritin is transported by, and remains bound to functional lymphatic vessels enabling histochemical localization using Prussian blue staining.<sup>23</sup> Consistent with our

lymphoscintigraphic findings, only obese C57BL/6J animals had significantly decreased lymph-node ferritin staining (twofold) as compared with their NCD-fed controls, whereas HFD-fed BALB/cJ and *MSTN<sup>ln</sup>* mice did not (Figures 2d and e).

Functional lymphatic vessels also regulate migration of antigen-presenting cells to regional lymph nodes where they interact with other immune cells.<sup>24</sup> Therefore, we analyzed migration of isolated DCs from the distal hindlimb (injection site) to the inguinal lymph node of HFD- and NCD-fed animals over a 24-h period. Flow cytometry of draining lymph nodes harvested from HFD-fed obese C57BL/6J mice demonstrated a more than 50% reduction in the number of trafficked DCs as compared with their NCD-fed controls (Figures 2f and g). In contrast, HFD-fed BALB/cJ and *MSTN<sup>ln</sup>* mice demonstrated no changes when compared with their NCD-fed controls. Taken together, these findings show that obesity, rather than simply prolonged exposure to HFD, is necessary for impaired lymphatic function in mice.

#### Obesity results in perilymphatic inflammation

We next analyzed tissues harvested from multiple anatomical locations and co-localized lymphatic vessels (LYVE-1<sup>+</sup>) with T cells (CD3<sup>+</sup>) or macrophages (CD11b<sup>+</sup>) since previous studies have shown that these inflammatory cell types have a key role in the regulation of pathological changes in obesity.<sup>3–6</sup> This approach enabled us to quantify perilymphatic inflammation, which we

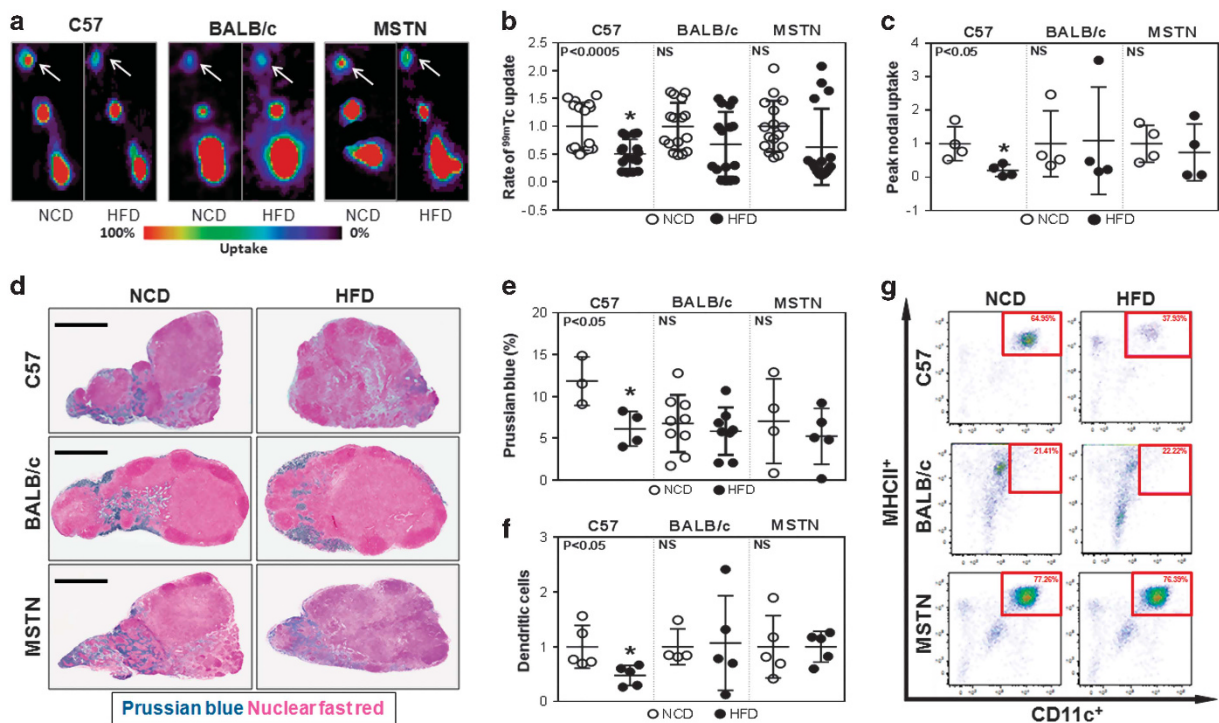


**Figure 2.** Obesity impairs lymphatic transport of macromolecules to draining lymph nodes. (a) Representative hindlimb <sup>99m</sup>Tc heat maps for NCD- and HFD-fed C57BL/6J, BALB/cJ and *MSTN<sup>ln</sup>* mice. White arrows indicate the uptake in the inguinal lymph nodes ( $n = 4$ /group). (b) Quantification of the rate of <sup>99m</sup>Tc uptake in inguinal lymph nodes following hindlimb injection. Data are presented as fold change relative to their NCD controls in each group ( $n = 16$ /group). C57BL/6J HFD vs NCD ( $*P < 0.0005$ ). *MSTN<sup>ln</sup>* and BALB/cJ had no significant difference between NCD and HFD groups. (c) Quantification of peak nodal uptake of <sup>99m</sup>Tc in inguinal lymph nodes following hindlimb injection. Data are presented as fold change relative to their NCD controls in each group ( $n = 4$ /group). C57BL/6J HFD vs NCD ( $*P < 0.05$ ). *MSTN<sup>ln</sup>* and BALB/cJ had no significant difference between NCD and HFD groups. (d) Representative Prussian blue-stained histological cross-sections of axillary lymph nodes harvested from NCD- or HFD-fed mice in all groups (scale bar = 500 μm). (e) Quantification of Prussian blue staining as a percentage of the total lymph-node area in NCD- and HFD-fed mice ( $n = 3–9$ /group). C57BL/6J HFD vs NCD ( $*P < 0.05$ ). *MSTN<sup>ln</sup>* and BALB/cJ had no significant difference between NCD and HFD groups. (f) Quantification of migrating CD45.1<sup>+</sup> DCs (MHCII<sup>+</sup>/CD11C<sup>+</sup>) in inguinal and popliteal lymph nodes of NCD- (open circles) and HFD- (filled circles) fed mice in all groups ( $n = 5$ /group). Data are presented as fold change from respective NCD-fed controls. C57BL/6J HFD vs NCD ( $*P < 0.05$ ). *MSTN<sup>ln</sup>* and BALB/cJ had no significant difference between NCD and HFD groups. (g) Representative dot plot graphs of inguinal/popliteal lymph node flow cytometry analyzing migrating CD45.1<sup>+</sup> DCs in all groups. Red square surrounds DC population.



defined as the number of inflammatory cells located within 50  $\mu\text{m}$  of a lymphatic vessel.

Analysis of ear tissues harvested from HFD-fed obese C57BL/6J mice demonstrated significant increases in the number of perilymphatic CD3<sup>+</sup> and CD11b<sup>+</sup> cells (3.6- and 3-fold increase from controls, respectively; Figures 3a and b, Supplementary Figure 2). Similar findings were noted in the trachea and back skin, suggesting that perilymphatic inflammation in obese C57BL/6J mice is a systemic phenomenon (Supplementary Figure 3). In contrast, HFD-fed BALB/cJ or MSTN<sup>fl/fl</sup> mice failed to show significant changes as compared with their NCD-fed controls, indicating that HFD alone is insufficient for perilymphatic inflammation.

Previous studies have shown that VEGF-C expression is increased in obese individuals and that this growth factor has a key role in macrophage infiltration and differentiation.<sup>25,26</sup> Consistent with these studies and our finding of increased macrophage infiltration in obese mice, we noted a marked increase in VEGF-C expression in both serum (1.75-fold) and skin (2-fold) of HFD-fed obese C57BL/6J mice, as compared with their NCD-fed controls (Figures 3c and d). In addition, analysis of skin tissues from obese HFD-fed C57BL/6J mice also demonstrated increased expression of inflammatory cytokines including TNF- $\alpha$  (20-fold) and IL-1 $\beta$  (8.32-fold) as compared with their NCD controls (Figures 3e and f).

Obesity downregulates expression of lymphatic markers in LECs  
We next analyzed gene expression in LECs isolated from the subcutaneous tissues of obesity-prone and obesity-resistant mice

fed either a HFD or a NCD. PCR analysis of sorted LECs isolated from obese HFD-fed C57BL/6J mice demonstrated a nearly twofold decrease in the expression of *Prox1* (a transcription factor necessary for lymphatic differentiation), *VEGFR-3* (a signaling receptor necessary for LEC proliferation and function) and *CCL21* (a chemotactic cytokine that regulates migration of DCs to lymphatic channels), as compared with their NCD-fed controls (Figure 4a). Immunofluorescent co-localization of lymphatic vessels (LYVE-1<sup>+</sup>) with *CCL21* confirmed our PCR findings demonstrating a marked reduction in *CCL21* expression in lymphatic vessels of HFD-fed obese C57BL/6J mice as compared with their NCD-fed controls (Figure 4b). Furthermore, LECs isolated from obese HFD-fed C57BL/6J mice demonstrated a more than twofold increase in the expression of the inflammatory cell receptor *ICAM-1* and the pro-apoptotic gene *Bax*. In contrast, we noted no significant gene expression changes in cell-sorted LECs isolated from HFD-fed BALB/cJ or MSTN<sup>fl/fl</sup> mice as compared with their respective NCD-fed controls.

Previous studies have shown that gradients of *CCL21* expression are necessary for migration of antigen-presenting cells (for example, DCs) to lymphatic channels.<sup>27,28</sup> In light of our observation that obese C57BL/6J mice had decreased DC trafficking and that their LECs had downregulated *CCL21* expression, we next sought to determine whether tissue gradients of *CCL21* expression are altered in obesity by analyzing protein levels in the skin and subcutaneous tissues. Interestingly, we found that cutaneous tissues harvested from HFD-fed C57BL/6J mice had a more than twofold increase in *CCL21* expression as compared with NCD-fed controls, suggesting

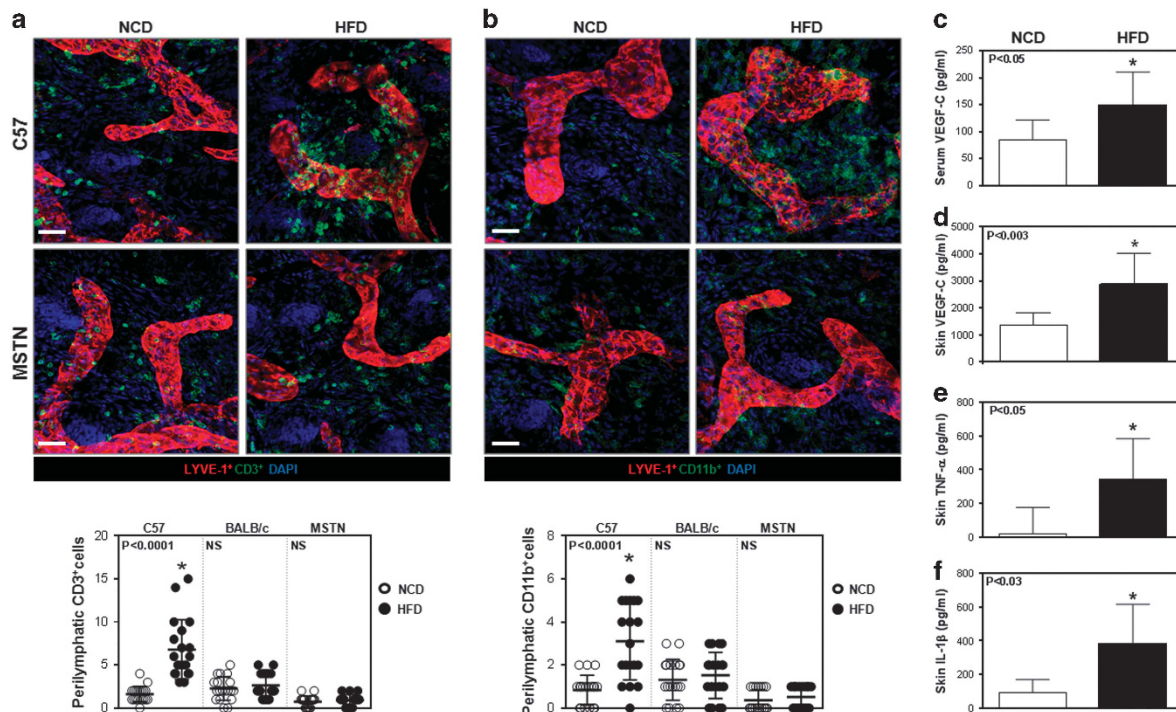


**Figure 3.** Obesity results in local tissue and perilymphatic inflammation. (a) Representative immunofluorescence co-localization (upper panel) of CD3<sup>+</sup> cells (green) and LYVE-1<sup>+</sup> vessels (red) in ear skin whole mounts harvested from NCD- and HFD-fed C57BL/6J and MSTN<sup>fl/fl</sup> mice. Blue stain is DAPI (scale bar = 30  $\mu\text{m}$ ). Quantification of perilymphatic CD3<sup>+</sup> cells in skin ear cross-sections of NCD- (open circles) and HFD- (filled circles) fed mice in all groups (lower panel). C57BL/6J HFD vs NCD ( $*P < 0.0001$ ,  $n = 4$  quadrants  $\times$  4–5 animals/group). MSTN<sup>fl/fl</sup> and BALB/cJ mice showed no significant difference between NCD and HFD groups. (b) Representative immunofluorescence co-localization (upper panel) of CD11b<sup>+</sup> cells (green) and LYVE-1<sup>+</sup> vessels (red) in ear skin whole mounts harvested from NCD- and HFD-fed C57BL/6J and MSTN<sup>fl/fl</sup> mice. Blue stain is DAPI (scale bar = 30  $\mu\text{m}$ ). Quantification of perilymphatic CD11b<sup>+</sup> cells in skin ear cross-sections of mice fed NCD (open circles) or HFD (filled circles) in all groups (lower panel). C57BL/6J HFD vs NCD ( $*P < 0.0001$ ,  $n = 4$  quadrants  $\times$  5 animals/group). MSTN<sup>fl/fl</sup> and BALB/cJ mice showed no significant difference between NCD and HFD groups. (c) Quantification of VEGF-C protein levels in serum harvested from lean and obese C57BL/6J mice ( $n = 10$ /group,  $*P < 0.05$ ). (d) Quantification of VEGF-C protein levels in back skin tissues harvested from lean and obese C57BL/6J mice ( $n = 6$ –10/group,  $*P < 0.003$ ). (e) Quantification of TNF- $\alpha$  protein levels in back skin tissues harvested from lean and obese C57BL/6J mice ( $n = 4$ –6/group,  $*P < 0.05$ ). (f) Quantification of IL-1 $\beta$  protein levels in back skin tissues harvested from lean and obese C57BL/6J mice ( $n = 5$ /group,  $*P < 0.03$ ).

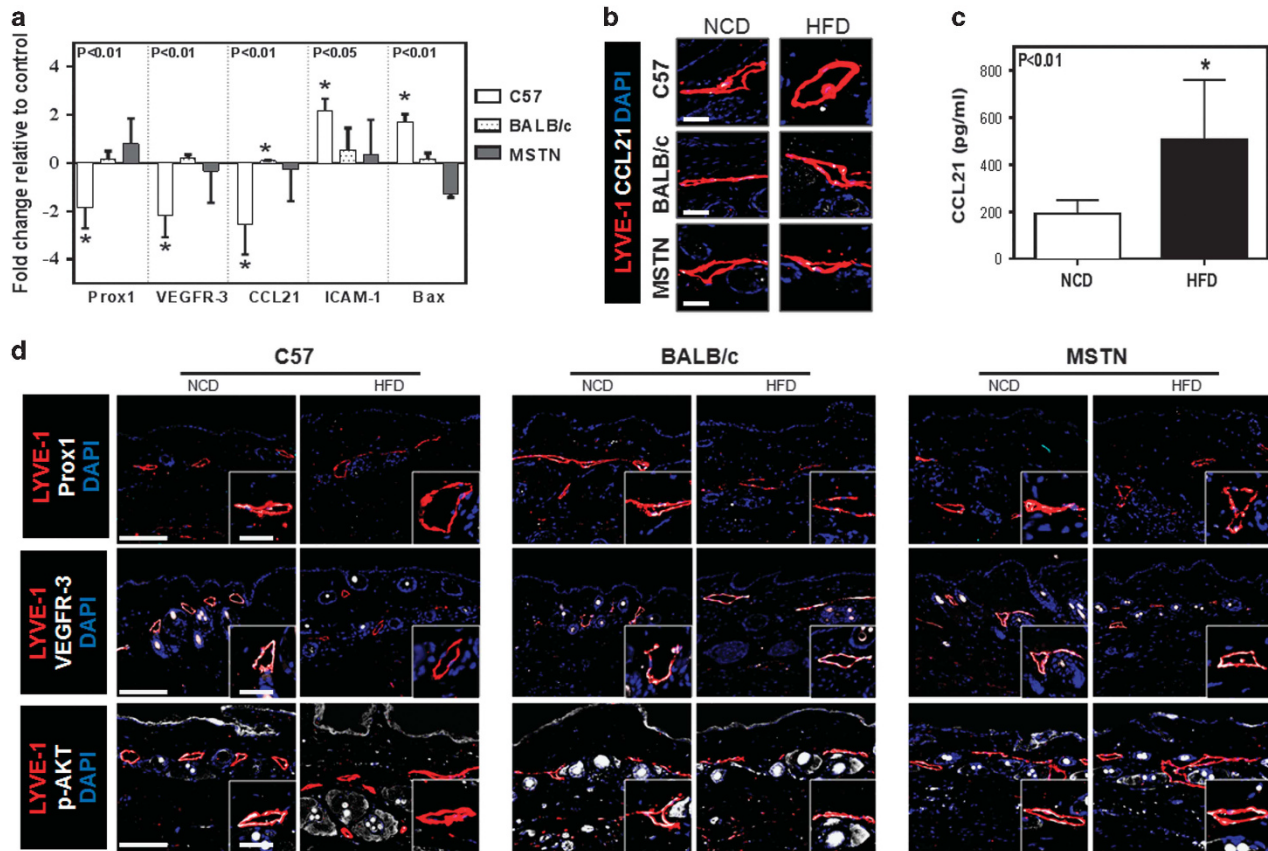


**Figure 4.** Obesity downregulates expression of lymphatic markers in LECs. (a) Quantification of mRNA expression in LECs sorted from NCD- and HFD-fed mice skin tissues for all groups, demonstrating relative expression of *Prox1*, *VEGFR-3*, *CCL21*, *ICAM-1* and *Bax* ( $n = 4-6$ /group). Data are presented as fold change relative to the NCD-fed controls in all groups. Note the downregulation of *Prox1*, *VEGFR-3* and *CCL21* ( $*P < 0.01$  for all) and the upregulation of *ICAM-1* ( $*P < 0.05$ ) and *Bax* ( $*P < 0.01$ ) in obese C57BL/6J when compared with their lean controls. (b) Representative immunofluorescent localization of LYVE-1<sup>+</sup>(red) and CCL21<sup>+</sup>(white) in NCD- and HFD-fed mice in all groups (DAPI is blue; scale bar = 25  $\mu$ m). (c) Quantification of CCL21 protein levels in hindlimb tissues harvested from lean and obese C57BL/6J mice ( $n = 6-8$ /group,  $*P < 0.01$ ). (d) Representative low and high power (dashed box shown in lower right inset) immunofluorescent localization of LYVE-1<sup>+</sup> cells (red) and Prox1 (top, white), VEGFR-3 (middle, white) and p-AKT (bottom, white) (DAPI nuclear stain is blue; scale bars = 50 and 25  $\mu$ m).

that clearance of inflammatory cells by the lymphatic system in obese animals is decreased, at least in part, due to a loss of gradients of CCL21 (that is, low expression in LEC and high expression in tissues) (Figure 4c).

To confirm our PCR findings, tissues were immunostained for LYVE-1 with VEGFR-3, Prox1 and p-AKT (a downstream mediator of VEGFR-3 signaling). Consistent with our PCR findings, we noted a marked decrease in VEGFR-3 and Prox1 expression by lymphatic vessels in HFD-fed obese C57BL/6J mice but not in HFD-fed BALB/cJ or MSTN<sup>fl</sup> mice (Figure 4d, Supplementary Figure 5). In addition, only the lymphatic vessels in obese C57BL/6J mice had a marked decrease in expression of p-AKT as compared with their lean controls.

Obesity results in perilymphatic lipid accumulation and *in vitro* exposure of LECs to FFA decreases cellular viability

We subsequently sought to identify potential mechanisms that may regulate LEC injury and gene expression changes in obesity. Previous studies have shown obesity results in macrophage accumulation, which subsequently engulf necrotic adipocytes resulting in the formation of 'crown-like structures' (CLS).<sup>29,30</sup> Adipocyte breakdown by CLS releases toxic by-products such as long-chain FFA, leading to increased expression of inflammatory mediators and worsening subcutaneous tissue inflammation.<sup>31,32</sup> Indeed, immunohistochemical analysis of skin harvested from obese HFD-fed C57BL/6J mice demonstrated the presence of CLS

in the subcutaneous fat (Figure 5a). Additionally, co-localization of lymphatic vessels (LYVE-1<sup>+</sup>) and lipids (BODIPY<sup>+</sup>) demonstrated the presence of numerous large lipid droplets in close proximity to LECs of obese HFD-fed C57BL/6J mice (Figure 5b). In contrast, we found little lipid accumulation in NCD-fed C57BL/6J controls.

We next performed corroborative *in vitro* studies on isolated LECs in order to better understand the effects of lipid by-products and FFA at the cellular level. SA is known to be increased in obesity where it has been shown to have toxic effects on blood endothelial cells.<sup>6,33</sup> We therefore compared the effects of SA on LECs with those on ASCs, as these cells are also present in adipose tissues. Interestingly, we found that SA, even in micromolar concentrations, was highly toxic to LECs resulting in a dose-dependent increase in cellular apoptosis as reflected by increasing activity of caspase-3 and annexin V (Figures 5c and d and Supplementary Figure 6A). In contrast, ASCs were highly resistant to SA-induced apoptosis or injury. In addition, similar to our PCR findings, we noted that exposing LECs to even low doses of SA resulted in a significant decrease in VEGFR-3 expression (threefold) as compared with LECs cultured in control media (Figures 5e and f). This is important since a major function of VEGFR-3 signaling in LECs is prevention of apoptosis through activation of AKT and subsequent downregulation of apoptotic pathways.<sup>34</sup>

VEGFR-3, similar to the insulin receptor, is a tyrosine kinase receptor (TKR) and activates intracellular signaling via a variety of mechanisms. A major intracellular signaling pathway of TKRs is



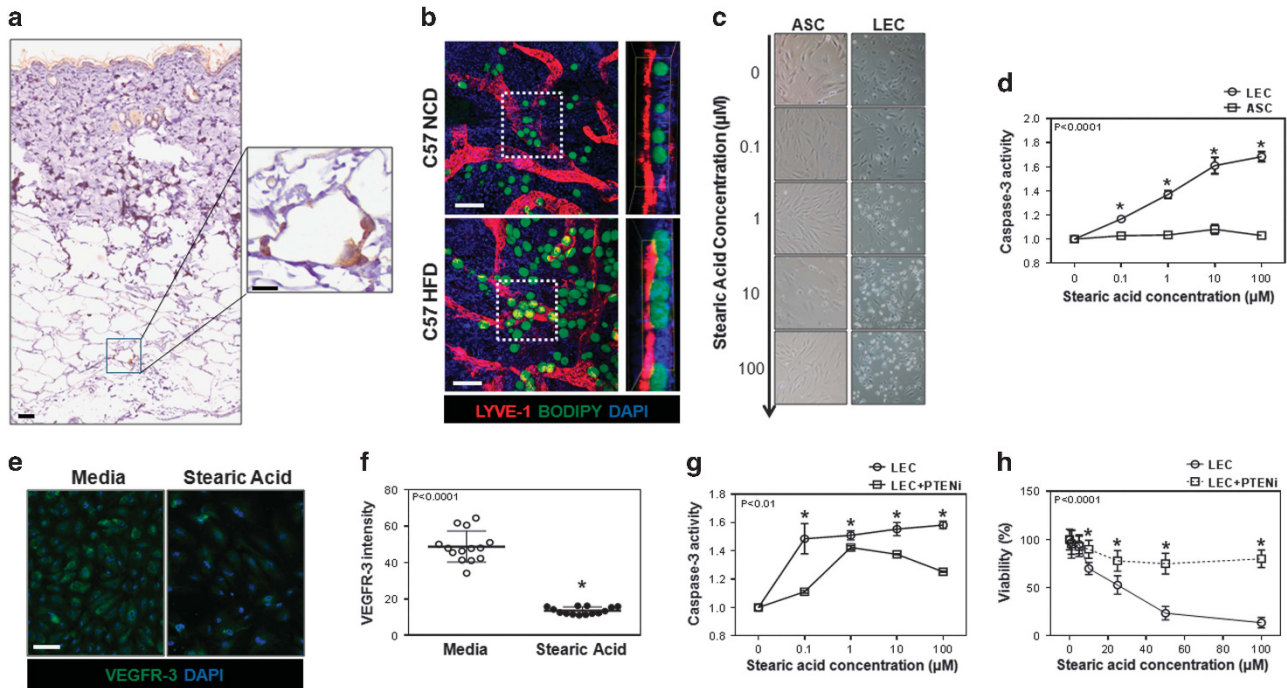


**Figure 5.** Obesity results in accumulation of large lipid droplets around lymphatic vessels. (a) Representative low (left) and high power (right) immunohistological localization of CD45<sup>+</sup> cells (brown) surrounding adipocytes (white) in back skin of obese C57BL/6J mice (scale bars = 100 and 25 μm, respectively). (b) Representative immunofluorescent localization (left) and orthoslice (right) from daughter region (white dotted square) of LYVE<sup>+</sup> cells (red), BODIPY<sup>+</sup> lipids (green) and nuclear DAPI stain (blue), in whole mount ear tissues of NCD- or HFD-fed C57BL/6J mice (scale bar = 20 μm). (c) Representative bright-field images showing LECs (top) and ASCs (bottom) cultured in media containing increasing concentrations of SA for 12 h. (d) Quantification of caspase-3 activity in LECs (circles) and ASCs (squares) after treatment with SA for 12 h ( $n = 3-5$ /group,  $*P < 0.0001$ ). (e) Representative immunofluorescent localization of VEGFR-3 expression (green) in LECs cultured with 10 μM of SA for 12 h (DAPI nuclear stain is shown in blue, scale bar = 25 μm). (f) Quantification of VEGFR-3 expression intensity in LECs cultured in media (open circle) or media with 10 μM SA (closed circle) for 12 h ( $n = 14$ /group,  $*P < 0.0001$ ). (g) Quantification of caspase-3 activity in LECs cultured with media containing SA (circle) or SA with 0.3 nM PTENi (square) for 12 h ( $n = 3$ /group,  $*P < 0.01$ ). (h) Quantification of LEC viability treated with media containing SA or SA with 0.3 nM PTENi for 12 h ( $n = 12$ /group,  $*P < 0.0001$ ).

regulated by phosphorylation of Phosphatidylinositol 4,5-bisphosphate (PIP2) to PIP3, which then activates downstream signaling pathways, including AKT phosphorylation. PTEN is an intracellular protein that dephosphorylates PIP3 to PIP2, thereby functioning as an intracellular inhibitor of VEGFR-3 signaling. To determine whether VEGFR-3 downregulation and subsequent decreased PIP3 activation in response to SA exposure have a causal role in increased apoptosis, we cultured LECs with SA, either with or without media supplemented with PTENi. Analysis of caspase-3 activity and cellular viability in these cells demonstrated a statistically significant protective effect of PTEN inhibition in LECs as compared with cells cultured without PTENi (Figures 5g and h). Similarly, we found that culturing isolated LECs with SA and either recombinant VEGF-C (direct activation of VEGFR-3 downstream pathways) or recombinant insulin (indirect activation of PIP3 pathway via tyrosine kinase activation) restored the viability of LECs cultured with SA (Supplementary Figure 6B).

Our VEGFR-3 immunocytochemistry findings were confirmed with western blot analysis of protein isolated from LECs cultured in media containing SA, with or without the addition of PTENi, VEGF-C or insulin (Figures 6a and b). Consistent with our immunocytochemistry findings, we noted that exposure of LECs to SA resulted in a 2.9-fold decrease in expression of VEGFR-3, a 3.7-fold decrease in expression of p-AKT and a 2.6-fold decrease in the expression of phosphorylated eNOS (p-eNOS, another downstream mediator of VEGFR-3). Addition of PTENi, recombinant VEGF-C or insulin to LECs cultured in media containing SA normalized VEGFR-3, p-AKT and p-eNOS expression to levels noted in LECs cultured in control (that is, no SA) media. Addition of PTENi, recombinant VEGF-C or insulin alone to LECs also significantly increased expression of these

proteins independent of SA, suggesting that intracellular PTEN function acts as a feedback mechanism regulating VEGFR-3 signaling.

Consistent with our cell-sorted PCR on LECs obtained from obese C57BL/6J mice, we noted a marked reduction in the expression of *Prox1* by LECs after exposure to SA (Figure 6c). This was normalized to control levels with the addition of PTENi, VEGF-C or insulin. We noted similar findings with Ki67 (a marker of cellular proliferation) and p-AKT expression. Taken together, our *in vitro* findings suggest that long-chain FFAs are harmful to LECs by decreasing the expression of master lymphatic regulators and that these effects can be mitigated by modulating intracellular pathways downstream of VEGFR-3 through PIP3 pathway and subsequently AKT activation.

## DISCUSSION

Previous clinical and laboratory studies have shown that obesity is a negative regulator of lymphatic function.<sup>3-10</sup> However, it remains unclear whether the observed effects on lymphatic function were secondary to weight gain, prolonged exposure to HFD or toxic metabolic by-products of adipose tissue. To address this question, we compared lymphatic function in obesity-prone and obesity-resistant mice after prolonged exposure to HFD. Our results are consistent with previous reports demonstrating that C57BL/6J mice become morbidly obese on HFD feeds,<sup>8,9</sup> while BALB/cJ and *MSTN<sup>fl/fl</sup>* mice do not<sup>21,22</sup> even though serum FFA levels were significantly increased in all HFD-fed mice.<sup>13,35</sup> This approach is clinically relevant as the incidence and severity of obesity in patients is also highly variable and modulated by genetic factors. Our findings imply that obesity, but not HFD, is necessary for the development of

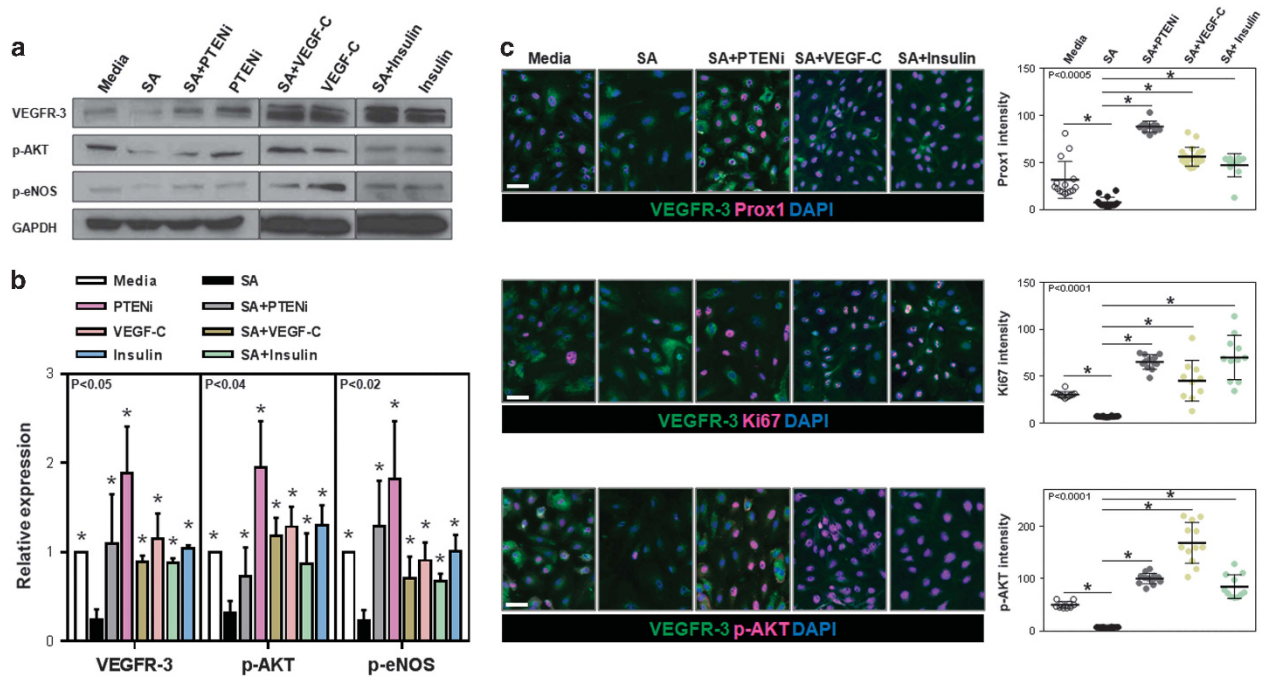


**Figure 6.** Exposure of LECs to SA *in vitro* downregulates expression of VEGFR-3 and its downstream mediators. **(a, b)** Representative western blot images **(a)** for VEGFR-3, p-AKT, p-eNOS and quantification **(b)** normalized to GAPDH expression of total cellular protein harvested from LECs treated with 1  $\mu\text{M}$  SA, 10  $\mu\text{M}$  SA+0.3 nM PTENi, PTENi (0.3 nM), SA+100 ng ml<sup>-1</sup> VEGF-C, VEGF-C (100 ng ml<sup>-1</sup>), SA+100 nM insulin or insulin (100 nM) ( $n=4-5/\text{group}$ ,  $*P < 0.05$  for all antibodies). **(c)** *Left panels:* Representative immunofluorescent co-localization of VEGFR-3 (green) and Prox1, Ki67 and p-AKT (all shown in pink) in LECs cultured in control media, media containing 10  $\mu\text{M}$  SA with PTENi (0.3 nM), 10  $\mu\text{M}$  SA with VEGF-C (100 ng ml<sup>-1</sup>) or 10  $\mu\text{M}$  SA with insulin (100 nM) for 12 h (scale bar = 25  $\mu\text{m}$ ). *Right panels:* Quantification of expression of Prox1, Ki67 and p-AKT in groups shown in the left panels ( $n=10-15/\text{group}$ ,  $*P < 0.0005$ ).

lymphatic dysfunction since obesity-resistant mice maintained essentially normal lymphatic function despite prolonged exposure to HFD feeds. Our study also suggests that obesity-induced tissue changes or alterations in glucose and/or FA metabolism (or a combination of all) are necessary for lymphatic dysfunction and that prolonged exposure to HFD alone does not cause direct injury to the lymphatic system.

Alternate hypotheses could explain the differences we noted in lymphatic function of obesity-prone and obesity-resistant mice after prolonged HFD feeds. For example, it is possible that strain-related differences may contribute to the disparities we observed in lymphatic function. Although our study does not definitely disprove this possibility, we believe that genetic differences in baseline lymphatic function are less important than the effects of obesity as *MSTN*<sup>fl</sup> mice are derived from a B6 background, and because *both* obesity-resistant mice strains (*MSTN*<sup>fl</sup> and BALB/cJ) were protected from lymphatic injury despite dissimilar genetic backgrounds. Additionally, although previous studies reported lymphatic dysfunction in ApoE-deficient mice with very high serum cholesterol levels (1000–2000 mg ml<sup>-1</sup>),<sup>36</sup> it is unlikely that changes in cholesterol levels are responsible for the lymphatic dysfunction we observed in our obese mice since the total cholesterol levels in our study were an order of a magnitude lower (< 200 mg ml<sup>-1</sup>) than those reported by Angeli *et al*. In addition, total and low-density lipoprotein cholesterol levels were elevated in all HFD-fed mice (that is, both obesity-prone and obesity-resistant mice). In fact, BALB/cJ mice had the highest serum levels of low-density lipoprotein cholesterol. Nonetheless, despite increases in total and low-density lipoprotein cholesterol in all HFD-fed animals, only the obese C57BL/6J mice displayed decreased lymphatic function indicating that modestly increased levels of cholesterol do not have deleterious effects on the lymphatic system.

A key histological difference between obesity-prone and obesity-resistant mice in our study was perilymphatic inflammation. This finding extends the results of previous studies demonstrating

chronic, low-grade perivascular inflammatory responses in obesity.<sup>37,38</sup> This is important because perivascular inflammation has a key role in the pathological outcomes of obesity on the blood vascular system by diverse mechanisms including altered expression of adipokines, impaired nitric oxide signaling and increased production of reactive oxygen species.<sup>7,39,40</sup> These effects are compounded by infiltration of macrophages that phagocytose necrotic adipocytes, leading to the release of long-chain FFA<sup>41</sup> that, in turn, have deleterious effects on endothelial cells.<sup>6,31,42</sup> Indeed, in our studies we observed the presence of numerous CLS, and close association of large lipid droplets with lymphatic vessels, in the subcutaneous tissues of obese mice. Thus, chronic perilymphatic inflammatory responses in obese animals may act via a variety of mechanisms to inhibit lymphatic function in this setting.

We analyzed gene expression changes in cell-sorted LECs from NCD and HFD mice, as well as isolated LECs cultured with SA, a long-chain fatty acid known to be increased in obesity.<sup>41</sup> This analysis demonstrated that obese animals (but not obesity-resistant mice fed a HFD) and LECs cultured with SA had markedly decreased expression of Prox1 and VEGFR-3. Consistent with this effect, we noted that LECs harvested from obese C57BL/6J mice had a marked increase in the expression of the pro-apoptotic gene *Bax* and decreased expression of p-AKT, the downstream mediator of VEGFR-3 activation. These findings are important as previous studies have shown that the transcription factor Prox1 is a master lymphatic regulator necessary for the maintenance of the lymphatic phenotype and VEGFR-3 expression.<sup>43</sup> Similarly, VEGFR-3 signaling has a crucial role in a variety of physiologic functions in LECs, including proliferation, migration, differentiation, protection from apoptosis and expression of nitric oxide.<sup>34,44</sup> To further explore the role of VEGFR-3 and TKR signaling in LEC response to injury, we cultured LECs with SA with or without an inhibitor of PTEN, VEGF-C or insulin. This analysis demonstrated that direct activation of VEGFR-3 signaling pathways with VEGF-C or indirect activation



of tyrosine kinase signaling with a PTEN inhibitor or insulin confers significant protective effects to LECs cultured with SA. Thus, downregulation of Prox1 and VEGFR-3 in obesity may serve as a key cellular mechanism regulating lymphatic dysfunction in this setting and represents a potential target for therapeutic interventions. Our findings also suggest that obesity or exposure to high levels of long-chain fatty acids decreases insulin sensitivity in LECs and that subsequent intracellular downregulation of tyrosine kinase activity (for example, AKT phosphorylation and eNOS) decreases LEC viability and proliferation.

A large number of studies have shown that inflammation increases lymphangiogenesis.<sup>45,46</sup> Thus, it may seem contradictory that we found decreased lymphatic vessel density in obese animals in which we also noted marked subcutaneous infiltration of T cells and macrophages. However, numerous other studies have shown that chronic inflammation in some physiologic settings can markedly inhibit lymphangiogenesis<sup>47,48</sup> and that the initial lymphangiogenic response to acute inflammation subsides over time.<sup>17,47,48</sup> Furthermore, these studies have shown that an important mechanism regulating this effect is decreased VEGFR-3 expression. For example, Huggenberger *et al.*<sup>49</sup> showed that chronic inflammation can decrease VEGFR-3 protein and gene expression during oxazolone challenge, despite concomitantly increased expression of pro-inflammatory cytokines TNF- $\alpha$ , IL-1 $\beta$  and IFN- $\gamma$ .<sup>49</sup> Others have reported that micro-RNAs regulate inflammation-induced decreased VEGFR-3 and Prox1 expression.<sup>50,51</sup> Finally, T cell-derived cytokines including IFN- $\gamma$ , IL-4 and IL-13 have been shown to directly inhibit lymphangiogenesis.<sup>46,52</sup>

Consistent with previous studies in obese mice and patients,<sup>26</sup> we noted a marked increase in VEGF-C expression in tissues and serum harvested from obese HFD-fed C57BL/6J mice. This effect has a key role on glucose homeostasis in obesity by regulating macrophage infiltration and differentiation.<sup>25</sup> In addition, the combination of increased VEGF-C in the context of decreased LEC VEGFR-3 expression in obese mice suggests that homeostatic mechanisms contribute to changes in VEGF-C expression. This scenario may be similar to insulin resistance in obesity (that is, increased insulin/decreased insulin receptor function), suggesting that similar mechanisms regulate lymphatic function, a condition we have termed *VEGF-C resistance*. Our hypothesis is supported by the fact that receptor downregulation/dysfunction is a common pathologic outcome in obesity, regulating sensitivity to a number of molecules including insulin and leptin.<sup>53,54</sup> In addition, VEGFR-3, similar to the insulin receptor, is a TKR,<sup>34</sup> and its expression in obesity may therefore be downregulated by similar mechanisms, including inflammatory cytokines<sup>55</sup> and FFAs.<sup>56</sup> Finally, similar to our findings in LECs *in vitro*, previous studies have shown that deletion of PTEN is protective against insulin resistance by increasing intracellular PI3K/AKT signaling.<sup>57</sup>

An important function of the lymphatic system is the transport of antigen-presenting cells to regional lymph nodes. In the current study, we found that obesity markedly decreases DC migration to regional lymph nodes and that this response may be related to decreased clearance of interstitial fluid as well as changes in gradients of CCL21 expression.<sup>27,58</sup> These findings are in-line with previous studies demonstrating decreased CCL21 gradients and increased LEC ICAM-1 expression in response to contact hypersensitivity.<sup>17</sup> Our findings are also consistent with the known roles of interstitial flow and VEGFR-3 expression in regulating CCL21 expression by LECs.<sup>59</sup> Thus, changes in CCL21 expression gradients and increased expression of ICAM by LECs may effectively trap antigen-presenting cells in peripheral tissues and prevent trafficking of activating or suppressive DCs to regional lymph nodes. These data suggest a new cellular mechanism that regulates impaired T-cell recall responses and may contribute to increased incidence of autoimmunity in obesity.<sup>60</sup>

In summary, we have shown that obesity, rather than prolonged exposure to HFD, is necessary for induction of lymphatic dysfunction in mice and that this response correlates with perilymphatic

inflammation and downregulation of LEC VEGFR-3 and Prox1 expression. In addition, we have shown that LECs are highly sensitive to the toxic effects of long-chain fatty acids that are known to be increased in obesity and that direct or indirect intracellular activation of PIP3 confers significant protection to LECs.

## CONFLICT OF INTEREST

The authors declare no conflict of interest.

## ACKNOWLEDGEMENTS

We thank Mesruh Turkekel, Navid Paknejad, Sho Fujisawa and Yevgeniy Romin of the Molecular Cytology Core at Memorial Sloan Kettering Cancer Center for assistance with both histology and tissue imaging (Core Grant (P30 CA008748)). This study was supported by NIH R01 HL11130-01 awarded to BJM, NIH T32 CA009501-26A1 grant to DAC, NIH T32 CA009501-27/28 grant to GGN, NIH/NCI Cancer Center Support Grant P30 CA008748, Plastic Surgery Foundation Pilot Research Grant awarded to JCG and GGN.

## REFERENCES

- 1 Ogden CL, Carroll MD, Kit BK, Flegal KM. Prevalence of childhood and adult obesity in the United States, 2011–2012. *JAMA* 2014; **311**: 806–814.
- 2 Cawley J, Meyerhoefer C. The medical care costs of obesity: an instrumental variables approach. *J Health Econ* 2012; **31**: 219–230.
- 3 Ross R. Atherosclerosis—an inflammatory disease. *N Engl J Med* 1999; **340**: 115–126.
- 4 Lumeng CN, Bodzin JL, Saltiel AR. Obesity induces a phenotypic switch in adipose tissue macrophage polarization. *J Clin Invest* 2007; **117**: 175–184.
- 5 Hajer GR, van Haeften TW, Visseren FL. Adipose tissue dysfunction in obesity, diabetes, and vascular diseases. *Eur Heart J* 2008; **29**: 2959–2971.
- 6 Harvey KA, Walker CL, Pavlina TM, Xu Z, Zaloga GP, Siddiqui RA. Long-chain saturated fatty acids induce pro-inflammatory responses and impact endothelial cell growth. *Clin Nutr* 2010; **29**: 492–500.
- 7 Cao H. Adipocytokines in obesity and metabolic disease. *J Endocrinol* 2014; **220**: T47–T59.
- 8 Weitman ES, Aschen SZ, Farias-Eisner G, Albano N, Cuzzzone DA, Ghanta S *et al.* Obesity impairs lymphatic fluid transport and dendritic cell migration to lymph nodes. *PLoS One* 2013; **8**: e70703.
- 9 Savetsky IL, Torrisi JS, Cuzzzone DA, Ghanta S, Albano NJ, Gardenier JC *et al.* Obesity increases inflammation and impairs lymphatic function in a mouse model of lymphedema. *Am J Physiol Heart Circ Physiol* 2014; **307**: H165–H172.
- 10 Savetsky IL, Albano NJ, Cuzzzone DA, Gardenier JC, Torrisi JS, Garcia Nores GD *et al.* Lymphatic function regulates contact hypersensitivity dermatitis in obesity. *J Invest Dermatol* 2015; **135**: 2742–2752.
- 11 Zawieja SD, Wang W, Wu X, Nepiyushchikh ZV, Zawieja DC, Muthuchamy M. Impairments in the intrinsic contractility of mesenteric collecting lymphatics in a rat model of metabolic syndrome. *Am J Physiol Heart Circ Physiol* 2012; **302**: H643–H653.
- 12 Lim RS, Kratzer A, Barry NP, Miyazaki-Anzai S, Miyazaki M, Mantulin WW *et al.* Multimodal CARS microscopy determination of the impact of diet on macrophage infiltration and lipid accumulation on plaque formation in ApoE-deficient mice. *J Lipid Res* 2010; **51**: 1729–1737.
- 13 Li M, Fu W, Li XA. Differential fatty acid profile in adipose and non-adipose tissues in obese mice. *Int J Clin Exp Med* 2010; **3**: 303–307.
- 14 Avraham T, Daluvoy S, Zampell J, Yan A, Haviv YS, Rockson SG *et al.* Blockade of transforming growth factor-beta1 accelerates lymphatic regeneration during wound repair. *Am J Pathol* 2010; **177**: 3202–3214.
- 15 Jolly K, Bradley F, Sharp S, Smith H, Mant D. Follow-up care in general practice of patients with myocardial infarction or angina pectoris: initial results of the SHIP trial. Southampton Heart Integrated Care Project. *Fam Pract* 1998; **15**: 548–555.
- 16 Aschen SZ, Farias-Eisner G, Cuzzzone DA, Albano NJ, Ghanta S, Weitman ES *et al.* Lymph node transplantation results in spontaneous lymphatic reconnection and restoration of lymphatic flow. *Plast Reconstr Surg* 2014; **133**: 301–310.
- 17 Vigl B, Aebischer D, Nitschke M, Iolyeva M, Rothlin T, Antsiferova O *et al.* Tissue inflammation modulates gene expression of lymphatic endothelial cells and dendritic cell migration in a stimulus-dependent manner. *Blood* 2011; **118**: 205–215.
- 18 Schmittgen TD, Livak KJ. Analyzing real-time PCR data by the comparative CT method. *Nat Protoc* 2008; **3**: 1101–1108.
- 19 Zampell JC, Yan A, Elhadad S, Avraham T, Weitman E, Mehrara BJ. CD4(+) cells regulate fibrosis and lymphangiogenesis in response to lymphatic fluid stasis. *PLoS One* 2012; **7**: e49940.



- 20 Li Y, Prasad A, Jia Y, Roy SG, Loison F, Mondal S *et al*. Pretreatment with phosphatase and tensin homolog deleted on chromosome 10 (PTEN) inhibitor SF1670 augments the efficacy of granulocyte transfusion in a clinically relevant mouse model. *Blood* 2011; **117**: 6702–6713.
- 21 Montgomery MK, Hallahan NL, Brown SH, Liu M, Mitchell TW, Cooney GJ *et al*. Mouse strain-dependent variation in obesity and glucose homeostasis in response to high-fat feeding. *Diabetologia* 2013; **56**: 1129–1139.
- 22 McPherron AC, Lee SJ. Suppression of body fat accumulation in myostatin-deficient mice. *J Clin Invest* 2002; **109**: 595–601.
- 23 Isaka N, Padera TP, Hagendoorn J, Fukumura D, Jain RK. Peritumor lymphatics induced by vascular endothelial growth factor-C exhibit abnormal function. *Cancer Res* 2004; **64**: 4400–4404.
- 24 Randolph GJ, Angeli V, Swartz MA. Dendritic-cell trafficking to lymph nodes through lymphatic vessels. *Nat Rev Immunol* 2005; **5**: 617–628.
- 25 Karaman S, Hollmen M, Robciuc MR, Alitalo A, Nurmi H, Morf B *et al*. Blockade of VEGF-C and VEGF-D modulates adipose tissue inflammation and improves metabolic parameters under high-fat diet. *Mol Metab* 2015; **4**: 93–105.
- 26 Gomez-Ambrosi J, Catalan V, Rodriguez A, Ramirez B, Silva C, Gil MJ *et al*. Involvement of serum vascular endothelial growth factor family members in the development of obesity in mice and humans. *J Nutr Biochem* 2010; **21**: 774–780.
- 27 MartIn-FonTeChA A, Sebastiani S, Hopken UE, Uguccioni M, Lipp M, Lanzavecchia *et al*. Regulation of dendritic cell migration to the draining lymph node: impact on T lymphocyte traffic and priming. *J Exp Med* 2003; **198**: 615–621.
- 28 Saeki H, Moore AM, Brown MJ, Hwang ST. Cutting edge: secondary lymphoid-tissue chemokine (SLC) and CC chemokine receptor 7 (CCR7) participate in the emigration pathway of mature dendritic cells from the skin to regional lymph nodes. *J Immunol* 1999; **162**: 2472–2475.
- 29 Murano I, Barbatelli G, Parisani V, Latini C, Muzzonigro G, Castellucci M *et al*. Dead adipocytes, detected as crown-like structures, are prevalent in visceral fat depots of genetically obese mice. *J Lipid Res* 2008; **49**: 1562–1568.
- 30 Cinti S, Mitchell G, Barbatelli G, Murano I, Ceresi E, Faloia E *et al*. Adipocyte death defines macrophage localization and function in adipose tissue of obese mice and humans. *J Lipid Res* 2005; **46**: 2347–2355.
- 31 Suganami T, Nishida J, Ogawa Y. A paracrine loop between adipocytes and macrophages aggravates inflammatory changes: role of free fatty acids and tumor necrosis factor alpha. *Arterioscler Thromb Vasc Biol* 2005; **25**: 2062–2068.
- 32 Suganami T, Tanimoto-Koyama K, Nishida J, Itoh M, Yuan X, Mizuarai S *et al*. Role of the Toll-like receptor 4/NF-kappaB pathway in saturated fatty acid-induced inflammatory changes in the interaction between adipocytes and macrophages. *Arterioscler Thromb Vasc Biol* 2007; **27**: 84–91.
- 33 Opie LH, Walfish PG. Plasma free fatty acid concentrations in obesity. *N Engl J Med* 1963; **268**: 757–760.
- 34 Coso S, Bovay E, Petrova TV. Pressing the right buttons: signaling in lymphangiogenesis. *Blood* 2014; **123**: 2614–2624.
- 35 Machado MV, Michelotti GA, Xie G, Almeida Pereira T, Boursier J, Bohnic B *et al*. Mouse models of diet-induced nonalcoholic steatohepatitis reproduce the heterogeneity of the human disease. *PLoS One* 2015; **10**: e0127991.
- 36 Lim HY, Rutkowski JM, Helft J, Reddy ST, Swartz MA, Randolph GJ *et al*. Hypercholesterolemic mice exhibit lymphatic vessel dysfunction and degeneration. *Am J Pathol* 2009; **175**: 1328–1337.
- 37 Nieman DC, Henson DA, Nehlsen-Cannarella SL, Ekkens M, Utter AC, Butterworth DE *et al*. Influence of obesity on immune function. *J Am Diet Assoc* 1999; **99**: 294–299.
- 38 Womack J, Tien PC, Feldman J, Shin JH, Fennie K, Anastos K *et al*. Obesity and immune cell counts in women. *Metabolism* 2007; **56**: 998–1004.
- 39 Greenstein AS, Khavandi K, Withers SB, Sonoyama K, Clancy O, Jeziorska M *et al*. Local inflammation and hypoxia abolish the protective anticontractile properties of perivascular fat in obese patients. *Circulation* 2009; **119**: 1661–1670.
- 40 Ketonen J, Shi J, Martonen E, Mervaala E. Periadventitial adipose tissue promotes endothelial dysfunction via oxidative stress in diet-induced obese C57Bl/6 mice. *Circ J* 2010; **74**: 1479–1487.
- 41 Neels JG, Olefsky JM. Inflamed fat: what starts the fire? *J Clin Invest* 2006; **116**: 33–35.
- 42 Kosteli A, Sagaru E, Haemmerle G, Martin JF, Lei J, Zechner R *et al*. Weight loss and lipolysis promote a dynamic immune response in murine adipose tissue. *J Clin Invest* 2010; **120**: 3466–3479.
- 43 Wigle JT, Harvey N, Detmar M, Lagutina I, Grosveld G, Gunn MD *et al*. An essential role for Prox1 in the induction of the lymphatic endothelial cell phenotype. *EMBO J* 2002; **21**: 1505–1513.
- 44 Dumont DJ, Jussila L, Taipale J, Lymboussaki A, Mustonen T, Pajusola K *et al*. Cardiovascular failure in mouse embryos deficient in VEGF receptor-3. *Science* 1998; **282**: 946–949.
- 45 Kataru RP, Jung K, Jang C, Yang H, Schwendener RA, Baik JE *et al*. Critical role of CD11b+ macrophages and VEGF in inflammatory lymphangiogenesis, antigen clearance, and inflammation resolution. *Blood* 2009; **113**: 5650–5659.
- 46 Savetsky IL, Ghanta S, Gardenier JC, Torrisi JS, Garcia Nores GD, Hesse GE *et al*. Th2 cytokines inhibit lymphangiogenesis. *PLoS One* 2015; **10**: e0126908.
- 47 Baluk P, Tammela T, Ator E, Lyubynska N, Achen MG, Hicklin DJ *et al*. Pathogenesis of persistent lymphatic vessel hyperplasia in chronic airway inflammation. *J Clin Invest* 2005; **115**: 247–257.
- 48 Johnson LA, Prevo R, Clasper S, Jackson DG. Inflammation-induced uptake and degradation of the lymphatic endothelial hyaluronan receptor LYVE-1. *J Biol Chem* 2007; **282**: 33671–33680.
- 49 Huggenberger R, Siddiqui SS, Brander D, Ullmann S, Zimmermann K, Antsiferova M *et al*. An important role of lymphatic vessel activation in limiting acute inflammation. *Blood* 2011; **117**: 4667–4678.
- 50 Jones D, Li Y, He Y, Xu Z, Chen H, Min W. Mirtron microRNA-1236 inhibits VEGFR-3 signaling during inflammatory lymphangiogenesis. *Arterioscler Thromb Vasc Biol* 2012; **32**: 633–642.
- 51 Kazenwadel J, Michael MZ, Harvey NL. Prox1 expression is negatively regulated by miR-181 in endothelial cells. *Blood* 2010; **116**: 2395–2401.
- 52 Kataru RP, Kim H, Jang C, Choi DK, Koh BI, Kim M *et al*. T lymphocytes negatively regulate lymph node lymphatic vessel formation. *Immunity* 2011; **34**: 96–107.
- 53 Zhou Y, Rui L. Leptin signaling and leptin resistance. *Front Med* 2013; **7**: 207–222.
- 54 Lee BC, Lee J. Cellular and molecular players in adipose tissue inflammation in the development of obesity-induced insulin resistance. *Biochim Biophys Acta* 2014; **1842**: 446–462.
- 55 Su D, Coudriert GM, Hyun Kim D, Lu Y, Perdomo G, Qu S *et al*. FoxO1 links insulin resistance to proinflammatory cytokine IL-1beta production in macrophages. *Diabetes* 2009; **58**: 2624–2633.
- 56 Hotamisligil GS, Arner P, Caro JF, Atkinson RL, Spiegelman BM. Increased adipose-tissue expression of tumor-necrosis-factor-alpha in human obesity and insulin-resistance. *J Clin Invest* 1995; **95**: 2409–2415.
- 57 Wijesekara N, Konrad D, Eweida M, Jefferies C, Liadis N, Giacca *et al*. Muscle-specific Pten deletion protects against insulin resistance and diabetes. *Mol Cell Biol* 2005; **25**: 1135–1145.
- 58 Ohl L, Mohaupt M, Czeloth N, Hintzen G, Kiafard Z, Zwirner J *et al*. CCR7 governs skin dendritic cell migration under inflammatory and steady-state conditions. *Immunity* 2004; **21**: 279–288.
- 59 Iwami D, Brinkman CC, Bromberg JS. Vascular endothelial growth factor c/vascular endothelial growth factor receptor 3 signaling regulates chemokine gradients and lymphocyte migration from tissues to lymphatics. *Transplantation* 2015; **99**: 668–677.
- 60 Aritomi K, Kuwabara T, Tanaka Y, Nakano H, Yasuda T, Ishikawa F *et al*. Altered antibody production and helper T cell function in mice lacking chemokines CCL19 and CCL21-Ser. *Microbiol Immunol* 2010; **54**: 691–701.



This work is licensed under a Creative Commons Attribution-NonCommercial-NoDerivs 4.0 International License. The images or other third party material in this article are included in the article's Creative Commons license, unless indicated otherwise in the credit line; if the material is not included under the Creative Commons license, users will need to obtain permission from the license holder to reproduce the material. To view a copy of this license, visit <http://creativecommons.org/licenses/by-nc-nd/4.0/>

© The Author(s) 2016

Supplementary Information accompanies this paper on International Journal of Obesity website (<http://www.nature.com/ijo>)